Understanding interactions in a complex world: Design and analysis of multi-species functional response experiments

Benjamin Rosenbaum[1,2,*], Jingyi Li[1,2], Myriam R. Hirt[1,2], Remo Ryser[1,2], Ulrich Brose[1,2]

1. EcoNetLab, German Centre for Integrative Biodiversity Research (iDiv), Halle-Jena-Leipzig, Germany
2. Institute of Biodiversity, Friedrich Schiller University Jena, Jena, Germany
* Corresponding author: benjamin.rosenbaum@idiv.de

Abstract

1. The functional response describes resource-dependent feeding rates of consumers. While models for feeding on a single resource species are well studied and supported by a large body of empirical research, consumers feeding on multiple resource species are ubiquitous in nature. However, feeding experiments designed for parameterizing multi-species functional responses (MSFR) are extremely rare, mainly due to logistical challenges and the non-trivial nature of their statistical analysis.
2. Here, we describe how these models can be fitted to empirical data in a Bayesian framework. Specifically, we address the problem of prey depletion during experiments, which can be accounted for through dynamical modeling. In a comprehensive simulation study, we test the effects of experimental design, sample size and noise level on the identifiability of four distinct MSFR models. Additionally, we demonstrate the method's versatility by applying it to a list of empirical datasets.
3. We identify experimental designs for feeding trials that produce the most accurate parameter estimates in two- and three-prey scenarios. Although noise can introduce systematic bias in parameter estimates, model selection performs surprisingly well, almost always identifying the correct model even for small datasets.
4. Our flexible method allows the simultaneous analysis of feeding experiments from both single- and multi-prey scenarios, either with or without prey depletion. This will help to improve our understanding of prey selectivity, prey switching and hence food web stability and biodiversity. Our approach equips researchers with the right statistical tools to improve the mechanistic understanding of feeding interactions in complex ecosystems.

Keywords: species interactions, food webs, predation, prey switching, prey preference, experimental design, Bayesian methods

Introduction

In ecological communities, species engage in diverse interactions, forming complex networks that underpin the functioning and resilience of ecosystems. In the realm of food web ecology, these interactions are characterized by trophic links between species. Understanding the constraints on the strength of these links, which determine the flow of energy and matter through ecological systems, is crucial for predicting community structure and ecosystem functioning.

Feeding rates are commonly captured by the "functional response", which describes consumption of prey based on their density. Since its introduction (Holling, 1959), numerous models have been proposed (Jeschke et al., 2002), with a sustained interest until today (Abrams, 2022; DeLong, 2021). The most prevalent versions of the functional response are the Holling type 2 $F(N) = \frac{aN}{1+ahN}$ and the Holling type 3 $F(N) = \frac{bN^2}{1+bhN^2}$ (Jeschke et al., 2004; Kalinkat et al., 2023), where a is an attack rate (the fraction of habitat cleared from prey per time), h is handling time (the time the predator needs to consume and digest the prey), and b is a constant. The type 3 form arises from the type 2, when attack rates themselves are density-dependent, i.e. the attack rate of a predator increases with prey density as $a = bN$, but also a generalized formulation $a = bN^q$ with a flexible exponent $q > 0$ exists. The occurrence of sigmoidal type 3 functional responses has been explained by learning behavior of the predator when confronted with a prey species more frequently, or switching behavior between different prey species (Murdoch & Oaten, 1975). The difference between the functional response types has gained particular importance due to their effects on population and food web stability (Kalinkat et al., 2023).

Although classical functional response models measure interactions of a predator with a single prey species, nature is more complex. Predators typically have a variety of prey options, and their feeding habits (and thus interaction strengths) are influenced not just by the abundance of one prey species but by the collective presence and density of all available prey (Abrams, 2022). For instance, the GATEWAy database of 290 food webs (Brose et al., 2019) contains 2,917 predators, of

which 92% are reported to feed on more than one prey species. Feeding rates on a focal resource are generally expected to decrease in the presence of alternative resources. Their mathematical descriptions $F_i\left(N_1,\ldots,N_m\right)$ of feeding on a species i depend not only density N_i, but also on other prey densities N_j ($j \neq i$), leading to multi-species functional responses (MSFR), (Gentleman et al., 2003; Koen-Alonso, 2007). MSFRs are capable of modeling important concepts such as prey preference (Chesson, 1983), switching (Murdoch, 1969) or optimal foraging (Holt, 1983), with implications for species coexistence and ecosystem stability. A plethora of MSFR models covering these topics have been proposed, with examples in (Baudrot et al., 2016; Gentleman et al., 2003; Morozov & Petrovskii, 2013; Ryabov et al., 2015; Stouffer & Novak, 2021; Vallina et al., 2014). To our knowledge, none of these simultaneously included (1) sigmoidal behavior in single-prey scenarios, (2) active prey switching (which cannot be predicted from single-prey information) in multi-prey scenarios, and (3) prey species-specific maximum feeding rates (e.g. due to differences in body size). Here, we developed a new flexible but still tractable MSFR with these features that generalizes previous models.

To empirically measure and parameterize these mathematical descriptions of functional responses, feeding trials in highly controlled experiments are commonly used (Griffen, 2021). In single-prey scenarios, typically one or more predator individuals are allowed to feed on a given prey density for a fixed period of time and numbers of eaten prey are recorded. Experiments are replicated along a gradient of prey densities and functional response models are fitted to the observed data of eaten vs. offered prey abundances. This allows parameterizing models, testing model formulations, and tackling questions of e.g. allometric scaling or temperature dependence (Daugaard et al., 2019; Kratina et al., 2022; Sohlström et al., 2021; Uszko et al., 2017). Numerous single-prey experiments have been conducted in recent decades. The FoRAGE database compiles more than 2,500 taxonomically diverse datasets of functional responses from 70 years covering terrestrial, marine and freshwater habitats (Uiterwaal et al., 2022).

In multi-prey scenarios, accurate parameterization of MSFRs is required, not least because they are the backbone of modern food web models (Gauzens et al., 2023; Martinez, 2020), which

currently use multi-species extensions of the Holling type 3 response. Here, population dynamics may be sensitive to parameters such as the exponent q, with drastic consequences for biodiversity (Williams & Martinez, 2004). However, empirical evidence remains extremely rare, see e.g. (Stouffer & Novak, 2021) and (Coblentz, 2020) for non-exhaustive lists of 30 and 20 multi-species datasets, respectively. While the collection and analysis of field data has occasionally been accomplished (Beardsell et al., 2022) and features its own difficulties, even experiments in highly controlled laboratory settings come with logistical and statistical challenges.

First, these models tend to be data-hungry with potentially hundred(s) of individual feeding trials, each requiring the counting of up to hundreds of prey individuals of different species. Second, after data collection researchers are required to perform some sort of nonlinear model fitting which might exceed a classical statistics curriculum. Here, two factors have been widely disregarded in the literature: experimental design and prey depletion. First, even for a two-prey scenario, there are endless possibilities to set up experiments with combinations of prey densities N_1 and N_2, i.e., how to arrange a given number of points $\left(N_1, N_2\right)$ in a rectangle $[0, N_{1,max}] \times [0, N_{2,max}]$. The potential effects of experimental design on the accuracy of parameter estimation have not been exploited yet. Second, we know from single-prey experiments that model fitting without correcting for prey depletion leads to biased estimates (Rosenbaum & Rall, 2018). If eaten prey are not replaced instantly, prey abundances and hence feeding rates are not constant over the course of an experiment, but decrease. In single-prey experiments, statistical methods accounting for prey depletion are available (Pritchard et al., 2017; Rosenbaum & Rall, 2018; Uszko et al., 2020) with closed-form solutions for simple models as the type 2 response. More complex formulations (e.g. the flexible type 3 response using $a = bN^q$) are treated by predicting prey density dynamically (i.e. time-dependent $N(t)$) via ordinary differential equations (ODEs). The rate of change $\frac{dN(t)}{dt} =- F(N(t))$ is expressed by the functional response, and the equation can be solved for $N(t)$ numerically (by a computer algorithm).

In multi-prey scenarios, biases might be exacerbated, since both prey species are depleted by the predator in a nonlinear and interdependent way over the course of an experiment, unless eaten prey items (of the correct species) are constantly replaced to keep densities fixed (which, besides the

logistical effort, would likely cause disturbances of the predator's foraging process). Here, we propose to fit ODE-based predictions of eaten prey to observed numbers of both prey species in a two-prey scenario, extending the approach from (Rosenbaum & Rall, 2018) to the multi-prey case. Feeding rates on both species decline dynamically due to decreasing prey availability. Any density-dependent MSFR model can be included in a coupled set of differential equations

$$\frac{dN_1(t)}{dt} = -F_1(N_1(t), N_2(t)) \qquad \text{(eq. 1a)}$$

$$\frac{dN_2(t)}{dt} = -F_2(N_1(t), N_2(t)) \qquad \text{(eq. 1b)}$$

which can be solved numerically to predict the number of prey $\left(N_1(T), N_2(T)\right)$ remaining at the end of the experiment with duration T, given the initial prey densities $\left(N_1(0), N_2(0)\right)$. Their difference yields predictions of eaten prey $\left(N_{E,1}, N_{E,2}\right)$, which are fitted to the observed data to estimate model parameters such as attack rates, handling times and preferences.

We here show how MSFR models can be fitted to empirical data and demonstrate the method's accuracy. We conducted a simulation study following a "virtual ecologist" approach (Zurell et al., 2010), by generating realistic datasets of experiments *in silico* with a predator feeding on two prey species without prey replacement, to answer two questions: First, whether MSFR model parameters can be estimated correctly by fitting ODE-based model predictions and, second, through which experimental design we can obtain the best parameter estimates. As test cases we used multi-prey extensions of the Holling type 2, type 3 and a prey switching model. In addition, we developed a new, more flexible MSFR that generalizes these models (Fig. 1). In a full factorial approach, we tested (1) these four MSFR models of increasing complexity on (2) six experimental designs with (3) five levels of sample size. (4) Data was simulated with three levels of noise. (5) Each of these combinations was replicated 500 times. We fitted ODE-based predictions to each of the resulting 180,000 datasets in R using Bayesian inference (Markov Chain Monte Carlo sampling, MCMC) with Stan (Stan Development Team, 2023), which has a built-in numerical ODE solver. Additionally, we investigated scenarios with a predator feeding on three prey species in 48,000 datasets. We complement the simulation study with test cases using published experimental datasets.

We find that parameters of our tested MSFR models are generally estimated accurately using our new approach. In high-noise scenarios, however, parameter estimates can be systematically biased, but model selection still identifies the correct model even in small datasets. We provide practical suggestions for experimental designs of two- and three-prey feeding trials, that yield the most accurate estimates across all scenarios. Additionally, we provide a detailed tutorial and ready-to-use R code to facilitate the method's application.

Materials and Methods

Multi-species functional response models

(Koen-Alonso, 2007) mechanistically derived a generalized form of the MSFR by dividing a predator's total foraging time into searching time and time spent handling prey individuals of m different species, following (Holling, 1959). Then, by expressing the capture rate (number of prey eaten divided by searching time) as $C_i = p_i a_i N_i$, where p_i is a dimensionless selection factor (possibly depending on all resource densities $N_1,..., N_m$) and a_i is the attack rate ($a_i N_i$ depending on N_i only), the feeding rate on species i reads

$$F_i\left(N_1,..., N_m\right) = \frac{p_i a_i N_i}{1+\sum_{k=1}^{m} p_k a_k h_k N_k} . \quad \text{(eq. 2)}$$

Keeping p_i and a_i as constants or making either of them density-dependent produces different classes of MSFRs, which collapse to either type 2 or type 3 responses in single-species scenarios, and can exhibit different types of prey switching in multi-species scenarios (Fig. 1).

Prey switching is defined through preferences $\phi_i = \frac{F_i/N_i}{\sum_{k=1}^{m} F_k/N_k}$ and their pairwise ratio $\varphi_{ij} = \frac{\phi_i}{\phi_j} = \frac{F_i/N_i}{F_j/N_j}$ (Gentleman et al., 2003; Koen-Alonso, 2007; Murdoch, 1969). If φ_{ij} is a constant and not density-dependent, then the composition of a predator's diet $\frac{F_i}{F_j} = \varphi_{ij}\frac{N_i}{N_j}$ is relative to the

proportion of available prey $\frac{N_i}{N_j}$. E.g., $\varphi_{ij} > 1$ would mean that species i is always preferred over species j and consumed more often than its relative abundance in the environment would predict. If, however, φ_{ij} is density-dependent, a transition from $\varphi_{ij} < 1$ to $\varphi_{ij} > 1$ is possible and a switch from relative avoidance to relative preference of species i can occur when the composition of available prey changes. Preferences and switching are called passive when they can be explained by single-species information alone (e.g. differences in species-specific attack rates). Active switching, on the other hand, requires multi-species information and cannot be predicted from single-species data alone (Gentleman et al., 2003).

Holling type 2 MSFR

In its simplest expression of eq. (2), we assume constant attack rates a_i and let all $p_i = 1$ fixed, which produces a multi-species Holling type 2 response (Fig. 1a)

$$F_i = \frac{a_i N_i}{1 + \sum_{k=1}^{m} a_k h_k N_k} \qquad \text{(eq. 3)}$$

, e.g. (Gentleman et al., 2003). Note that we could not estimate free constants p_i and a_i both from data since they only appear as a product $a_i p_i$ in eq. (2). Estimates would be perfectly negatively correlated and therefore unidentifiable. In single-prey scenarios (all $N_j = 0, j \neq i$), the response collapses to the hyperbolic Holling-2 FR $F_i = \frac{a_i N_i}{1 + a_i h_i N_i}$. This MSFR does not produce prey switching, because relative prey preferences $\varphi_{ij} = \frac{a_i}{a_j}$ are constant and the ratio of attack rates determines relative prey preference or avoidance. Consequently, the MSFR is determined by single-prey parameters a_i and h_i, and could theoretically be estimated from single-prey feeding trials alone.

Holling type 3 MSFR

Allowing attack rates $a_i = b_i N_i^q$ to be density-dependent with a coefficient b_i and a positive exponent q, while still keeping all $p_i = 1$ fixed, generates a multi-species Holling type 3 response (Fig. 1b)

$$F_i = \frac{b_i N_i^{1+q}}{1+\sum_{k=1}^{m} b_k h_k N_i^{1+q}} \qquad \text{(eq. 4)}$$

, e.g. (Gentleman et al., 2003). In single-prey scenarios, the response collapses to a sigmoidal Holling-3 FR $F_i = \frac{b_i N_i^{1+q}}{1+b_i h_i N_i^{1+q}}$, which is associated with more stable dynamics than a type 2 FR even for small values of q (Kalinkat et al., 2023). Relative prey preferences $\varphi_{ij} = \frac{b_i}{b_j}\left(\frac{N_i}{N_j}\right)^q$ are density-dependent for all $q > 0$ and can produce prey switching. Since all parameters (b_i, h_i, q) could theoretically be estimated from single-prey data, switching is passive.

Yodzis MSFR

For another MSFR (Koen-Alonso & Yodzis, 2005), named Yodzis functional response in (Koen-Alonso, 2007), selection factors $p_i = \frac{w_i N_i^r}{\sum_{k=1}^{m} w_k N_k^r}$ are made density-dependent (for positive $r > 0$), while attack rates a_i are constants. The denominator ensures $\sum_{k=1}^{m} p_k = 1$ independent of prey composition, and dimensionless preference weights are required to satisfy $\sum_{k=1}^{m} w_k = 1$. It can be written as

$$F_i = \frac{w_i a_i N_i^{1+r}}{\sum_{k=1}^{m} w_k N_k^r + \sum_{k=1}^{m} w_k a_k h_k N_k^{1+r}}, \qquad \text{(eq. 5)}$$

see Fig. 1c. For $r = 0$ it reduces to a Holling-2 MSFR (replacing $w_i a_i$ by a_i). In single-prey scenarios it collapses to a Holling-2 FR even for positive $r > 0$, which cancels out just like the weights w_i. In multi-prey scenarios however, prey switching can occur because the relative preference

$\varphi_{ij} = \frac{w_i a_i}{w_j a_j}\left(\frac{N_i}{N_j}\right)^r$ is density-dependent, with exponent r controlling the abruptness of switching. Single-prey data does not hold any information on parameters w_i and r. Therefore, information from multi-prey scenarios is required to fully determine this MSFR, making it an active-switching response.

Generalized switching MSFR

Finally, we can make both the attack rates $a_i = b_i N_i^q$ and the selection factors $p_i = \frac{w_i N_i^r}{\sum_{k=1}^{m} w_k N_k^r}$ density-dependent. This new MSFR (Fig. 1d)

$$F_i = \frac{w_i b_i N_i^{1+q+r}}{\sum_{k=1}^{m} w_k N_k^r + \sum_{k=1}^{m} w_k b_k h_k N_k^{1+q+r}} \qquad \text{(eq. 6)}$$

generalizes the three previous models. For $q = r = 0$ it reduces to a Holling-2 MSFR (replacing $w_i b_i$ with a_i), for $q > 0$ and $r = 0$ it reduces to a Holling-3 MSFR (replacing $w_i b_i$ by b_i), and for $q = 0$ and $r > 0$ it reduces to the Yodzis MSFR (replacing b_i by a_i). It collapses to a type 3 FR in single-prey scenarios, but unlike the Holling-3 MSFR, the switching is active: relative preference $\varphi_{ij} = \frac{w_i b_i}{w_j b_j}\left(\frac{N_i}{N_j}\right)^{q+r}$ is density-dependent and parameters w_i and r can only be informed with multi-prey data. While $q > 0$ controls the sigmoidal shape in single-prey scenarios, switching can be even more pronounced in multi-prey scenarios via the exponent $q + r$.

Experimental design

We tested six experimental designs for combining initial abundances of two prey species (Fig. 2). The maximum abundance of each species was 200. Abundances were always rounded to the nearest integer. For each design, we tested numbers of *n* = 64, 128, 256, 512 and 1024 feeding trials.

1. Random design. For each feeding trial, abundances $N_{0,1}$ and $N_{0,2}$ are each drawn from a uniform distribution $U(0, 200)$.
2. Space-filling design. We use a Halton sequence, a quasi-random number sequence that covers a rectangle more evenly than a purely random distribution (R-package "randtoolbox" (Dutang & Savicky, 2023)).
3. Grid. Abundances are placed equidistantly on an 8x8 factorial grid. 1, 2, 4, 8 or 16 replicates of each combination were used to achieve given sample sizes *n*.
4. Log-spaced grid. Distances between grid points are not identical, but increase by factor 1.5 with increasing abundance. Thus, more experiments are distributed at lower abundance levels. Again, we used 1, 2, 4, 8 or 16 replicates of each combination.
5. Triangle. Feeding trials are conducted in single-prey scenarios for each species (*n*/4 trials each, equidistant), and on a diagonal line in multi-prey scenarios (*n*/2 trials, equidistant), where the total number of initially available prey $N_{0,1} + N_{0,2} = 200$ is constant.
6. Diagonals. Experiments are placed equidistantly along 8 diagonals, each representing a different constant level of total prey $N_{0,1} + N_{0,2}$ (*n*/8 experiments each).

Data simulation

For each simulated dataset, model parameters were drawn from random distributions to represent a unique combination of a predator and two prey species. **First**, we sampled maximum feeding rates $f_{max,i} \sim U(50, 100)$ and half-saturation densities $N_{half,i} \sim U(25, 75)$ of each species ($i = 1, 2$) from uniform distributions. This determines handling times $h_i = \frac{1}{f_{max,i}}$ and attack rates $a_i = \frac{f_{max,i}}{N_{half,i}}$ (Holling-2 and Yodzis-FR), or attack coefficients $b_i = \frac{f_{max,i}}{N_{half,i}^{1+q}}$ (Holling-3 and Generalized-FR), see e.g. (Rosenbaum & Rall, 2018). Exponents $q \sim U(0.5, 1.5)$ (Holling-3 and Generalized-FR) and $r \sim U(0.5, 1.5)$ (Yodzis-FR and Generalized-FR) were also drawn randomly and determined varying strengths of prey switching. Preference weights (w_1, w_2) were sampled from a joint Dirichlet

distribution satisfying $w_1 + w_2 = 1$, with its shape parameters $(3, 3)$ describing the level of concentration towards to their mean $(0.5, 0.5)$.

Second, for each feeding trial $j = 1,..., n$ of a given experimental design, we deterministically predicted the mean density of eaten prey $(N^*_{E,1}, N^*_{E,2})_j$. We numerically solved the coupled differential equations (eq. 1) with initial densities $(N_{0,1}, N_{0,2})_j$ after a generic experimental duration of $T = 1.0$ using the R-package "deSolve" (Soetaert et al., 2010) and computed $N^*_{E,i,j} = N_{0,i,j} - N^*_{T,i,j}$ $(i = 1, 2)$. The range of parameters chosen above resulted in predator saturation levels $\frac{N^*_{E,i,j}}{f_{max,i}}$ in single-prey experiments at the highest available densities $N_{0,i} = 200$ of 78% (Holling-2 and Yodzis-FR) and 91% (Holling-3 and Generalized-FR) on average with a standard deviation of 5%, each.

Third, because feeding events happen randomly, we allowed for random variation around the predicted means $N^*_{E,i,j}$ by drawing the final integer numbers of eaten prey items $N_{E,i,j}$ from Binomial distributions with $N_{0,i,j}$ trials and success probability $\frac{N^*_{E,i,j}}{N_{0,i,j}}$. Here, $N_{E,i,j}$ are bounded between 0 and $N_{0,i,j}$.

With this level of randomness we observed coefficients of variation (CV, standard deviation divided by mean) of 0.11 on average (95% quantiles [0.08,0.15]) in simulated single-prey experiments in highest available densities $N_{0,i} = 200$ (Fig. 3). However, variation in experimental datasets can be higher. E.g., (Uszko et al., 2020) observed CVs between 0.31 to 0.58 in feeding experiments for aquatic and terrestrial invertebrates.

To increase the noise in simulated datasets to more realistic levels, we acknowledge that each study usually includes multiple predator individuals that may differ in their morphological and physiological traits, e.g. body size (DeLong, 2021; DeLong et al., 2021). We assumed that each trial ($j = 1,..., n$) is conducted with one predator individual, which is not reused in multiple trials. In the approach described above, all predators' traits were identical to the population-level means as described by parameters such as attack rates a_i and handling times h_i (for prey species $i = 1, 2$).

Then, we allowed intraspecific trait variation around the population-level means for attack rates $a_{i,j} \sim N(a_i, \sigma a_i)$ (Holling-2 and Yodzis-FR; same for $b_{i,j}$, Holling-3 and Generalized-FR) and handling times $h_{i,j} \sim N(h_i, \sigma h_i)$, where σ describes the relative amount of variation. In addition to the above case ($\sigma = 0$), we tested $\sigma = 0.2$ and $\sigma = 0.4$, which produced CVs of 0.20 on average (95% quantiles [0.17,0.24]) and 0.40 (95% quantiles [0.34,0.50]), respectively (Fig. 3). Here, noise originates both from variability in traits between individuals (and therefore between trials) and from additional Binomial error due to the randomness of feeding events in each trial.

Statistical approach

We combined numerical ODE simulations with Bayesian inference to estimate model parameters θ (e.g., $\theta = (a_1, a_2, h_1, h_2)$ for Holling-2) from datasets of initial prey abundances $(N_{0,1}, N_{0,2})_j$ and observed numbers of eaten prey $(N_{E,1}, N_{E,2})_j$, $j = 1,..., n$. We used the R-package "rstan" (Stan Development Team, 2023) to sample from the posterior probability distribution $P(\theta|Y) \sim P(Y|\theta)P(\theta)$ of model parameters θ given the data Y, where $P(Y|\theta)$ is the likelihood function connecting model predictions with data, and $P(\theta)$ is a prior distribution for the parameters. In each MCMC iteration, model predictions for eaten prey $N^*_{E,i,j} = N_{0,i,j} - N^*_{T,i,j}$ $(i = 1, 2)$ are computed by numerical integration of the coupled equations (1) in $t \in [0, T]$ with initial densities $(N_{0,1}, N_{0,2})_j$ using Stan's built-in ODE solver. We chose a Binomial distribution $N_{E,i,j} \sim Binomial(n = N_{0,i,j}, p = \frac{N^*_{E,i,j}}{N_{0,i,j}})$ as likelihood function.

As prior distributions we chose exponential distributions with rate 1.0 for parameters a_i, b_i, q, r and rate 10.0 for h_i, with mean and standard deviation given by the inverse of the rate. Preference weights (w_1, w_2) were coded as two-dimensional simplex vectors with a Dirichlet distribution and its shape parameters $(2, 2)$ as prior distribution to ensure $w_1 + w_2 = 1$. These

vaguely informative priors merely represent the parameters' order of magnitude, as not to confound results on estimation accuracy with prior information.

Each model was fitted using 1,000 warmup steps and 2,000 samples in three chains, adding up to 6,000 samples of the parameters' posterior distribution. We discarded datasets when the MCMC did not converge properly (more than 100 divergent iterations).

Evaluation

To evaluate the accuracy of each model fit we compared metrics of parameter estimates $\widehat{\theta}$, given by their posterior probability distribution $P(\widehat{\theta}|Y)$, and the known true parameters θ which generated the dataset (Lotterhos et al., 2022). Relative bias

$$Bias(\widehat{\theta}_k) = \frac{1}{\theta_k}\left(E(\widehat{\theta}_k) - \theta_k\right) \qquad \text{(eq. 7)}$$

is a measure of how much a parameter's point estimate, posterior mean $E(\widehat{\theta}_k)$, deviates from the true value (accuracy). Relative root mean squared error

$$RMSE(\widehat{\theta}_k) = \frac{1}{\theta_k}\sqrt{\left(E(\widehat{\theta}_k) - \theta_k\right)^2 + Var(\widehat{\theta}_k)} \qquad \text{(eq. 8)}$$

also accounts for the uncertainty of the estimate, expressed by posterior variance $Var(\widehat{\theta}_k)$ (precision). To summarize this information for each fit, single metrics were computed through geometric means of the individual parameters' RMSEs

$$\overline{RMSE} = \prod_{k=1}^{K} RMSE(\widehat{\theta}_k)^{1/K}. \qquad \text{(eq. 9)}$$

Model comparison

We tested whether not only true model parameters could be accurately recovered by fitting the same MSFR model that generated the dataset, but also whether the correct model could be identified among other model candidates. For the data from designs that produced the most accurate estimates as

described in the previous section (log-spaced grid), we additionally fitted all four model candidates to each dataset and performed model selection. We used the leave-one-out cross-validation (LOO-CV) method via the R-package “loo” (Vehtari et al., 2023). The model associated with the lowest information criterion was selected as the best fitting model. However, if the difference in model performance was less than two standard deviations of the included uncertainty, the less complex model was selected according to the principle of parsimony (ranking Holling-2 < Holling-3 < Yodzis-FR < Generalized-FR in complexity).

Three-prey scenarios

Additionally, we tested scenarios with a predator feeding on three prey species. All of the above methods can be easily extended to models, simulations and fittings with more than two prey species. We wanted to know if feeding trials involving all three prey species simultaneously are required to accurately estimate model parameters, or if pairwise combinations of two-prey feeding trials are sufficient. The log-spaced grid design, which performed best in the study described above, was extended to

1. a full factorial three-dimensional 7×7×7 grid
2. three 8×8 grids with species combinations (1,2), (1,3) and (2,3),

see Fig. S12. Subtracting single-prey trials that would occur twice, the pairwise trials sum up to $3\times8^2–3\times8=168$ unique combinations of prey abundances, which were replicated 1, 2, 4 and 6 times to generate sample sizes *n* of 168, 336, 672 and 1008. The full factorial trials total $7^3=343$ unique combinations, which were replicated 1, 1, 2 and 3 times (343, 343, 686, 1029) and randomly downsampled to the four sample sizes of the pairwise designs, respectively, for comparability. Data was generated for all four MSFR models and all three noise levels. All parameter ranges were as described above in the two-prey scenarios. Again, 500 replicates of each scenario were generated and fitted, summing up to 48,000 datasets.

Empirical datasets

We analyzed 23 datasets from 10 publications, including 5 studies from the list of (Stouffer & Novak, 2021) and 5 recent studies, see Table S1 for a full list of datasets. We required datasets to include both single- and two-prey experiments, and some variation in offered relative prey abundances $N_{0,1}/N_{0,2}$. For two studies that did not include raw data but summary statistics of eaten prey, we replicated full datasets. Numbers of individual feeding trials ranged from 48 to 290. Experiments had been conducted either without or with prey replacement, and two studies also included a mixture of both. In case of prey replacement, feeding rates were assumed to be constant during the whole experiment. We fitted direct predictions $N_{E,i} = F_i(N_{0,1}, N_{0,2}) \cdot T\ (i = 1, 2)$ instead of ODE predictions, and used a Poisson likelihood instead of a Binomial likelihood function. Bayesian modeling allowed these two types of observations to be combined in one statistical model for the two studies with mixed data. We performed model selection as described above to determine the best fitting MSFR for each dataset.

Results

We observed good convergence of the MCMC algorithm when fitting simulated data (100% of all fits for Holling-2 and Holling-3, 99.8% Yodzis-FR, 98% Generalized-FR). Runtime ranged between a couple of minutes for the smallest and several hours for the largest datasets.

Experimental design

We first assessed through which experimental design we could obtain the most accurate parameter estimates. Overall, experiments with the log-spaced grid resulted in smallest estimation errors in terms of RMSE for all four MSFRs and all levels of sample size and noise. Fig. 4 shows results for intermediate noise scenarios, but similar trends were observed in all three noise scenarios (Figs. S5-S7). In general, estimation performance increased with sample size as expected. But the choice of design was so influential that it could outperform other designs with twice the amount of feeding

trials, e.g. log-spaced grid vs. a random or a space-filling design for Yodzis-FR and the Generalized-FR (Fig. 4c,d). For these two active switching MSFRs, the difference between the log-spaced grid and other designs was also the most pronounced.

In many scenarios, the random and the space-filling designs performed worst. These were the only designs that do not explicitly include single-prey experiments (except by random chance), suggesting that experiments with mixed two-prey feeding trials only should be avoided.

The triangle design gave mixed results, e.g. performing second best for Yodzis-FR but worst for Holling-3. Such designs are common in the literature (Stouffer & Novak, 2021). They are suitable for analyzing two-prey feeding data with generalized linear models (GLMs) by relating the proportion of species 1 consumed $\frac{N_{E,1}}{N_{E,1}+N_{E,2}}$ to the proportion of species 1 available $\frac{N_{0,1}}{N_{0,1}+N_{0,2}}$, while the total amount of offered prey $N_{0,1} + N_{0,2}$ is constant for the mixed-prey scenarios, e.g. (McCard et al., 2021). In general, for all four MSFR models the proportion of feeding rates $\frac{F_1}{F_1+F_2}$ vs. proportion of prey availability $\frac{N_{0,1}}{N_{0,1}+N_{0,2}}$ is independent of total prey number $N_{0,1} + N_{0,2}$ (increasing both $N_{0,1}$ and $N_{0,2}$ by a factor c increases $N_{0,1} + N_{0,2}$ by factor c, which cancels out in $\frac{N_{0,1}}{N_{0,1}+N_{0,2}}$ and in $\frac{F_1}{F_1+F_2}$). However, this only holds when prey abundance is constant throughout the whole feeding trial, whereas for ODE predictions (and experiments without prey replacement) $\frac{N_{E,1}}{N_{E,1}+N_{E,2}}$ depends on total prey abundance $N_{0,1} + N_{0,2}$ (Fig. S8). We conclude that two-prey experiments with a fixed sum of available prey abundances alone, i.e. along one diagonal, are not necessarily representative of all combinations of prey abundances.

From here on, all results will be presented for the best performing design, log-spaced grid, only.

Intraspecific variation effects

Second, we tested how noise (caused by the predator's intraspecific trait variation) affected estimation performance (Fig. 5). Estimates generally worsened with increasing noise as expected. They improved with sample size in low- and medium-noise scenarios. In high-noise scenarios, however, estimates did not improve much on average with increasing sample size after a certain threshold was reached, e.g. comparing the average performance of datasets with 512 and 1024 feeding trials.

This is because parameter estimates can be systematically biased in these high-noise datasets (Figs. S1-S4). Handling times were, on average, underestimated for all four MSFR models. Attack rates were also underestimated on average (Holling-2 and Yodzis-FR). For Holling-3 and the Generalized-FR, attack coefficients were overestimated, while their exponents were underestimated. Negative bias in exponents generally lead to underestimated attack rates $a = bN^q$, too.

These systematic biases can be traced back to Jensen's inequality for nonlinear functions: Variation in individual attack rates lowers mean feeding (mostly at low to intermediate abundances) and variation in handling times increases mean feeding (at high abundances), see (Bolnick et al., 2011) and Fig. S9. Fitting population-level mean parameters must necessarily compensate for this by underestimating feeding rates at low abundances (by underestimating attack rates or attack exponents) and overestimating feeding rates at high abundances (by underestimating handling times).

Additionally, we tested whether alternative likelihood functions that account for this overdispersion in the data could mediate these biases. We used the Negative Binomial and the Beta Binomial distribution (Fenlon & Faddy, 2006). Although these distributions account for higher variance in the data, their estimation performance was even worse than that of the Binomial distribution (Fig. S10). They all fit population-level mean feeding rates through population-level mean trait parameters, which are not identical. We hypothesize that overdispersion parameters introduce additional degrees of freedom, which may worsen estimation performance, while not solving the problem of Jensen's inequality.

Model comparison

Although true parameter values could mostly not be identified without bias in high-noise scenarios, model selection was almost always able to identify the model used to simulate the data from the four candidate models (Fig. S11). Importantly, this result was independent of noise, and even small datasets (n=64) were sufficient to select the correct model in more than 98% of the cases (with only one exception: the most complex MSFR was correctly identified in only 90% of the cases for the smallest sample size n=64).

Three-prey scenarios

Estimation errors (RMSE) generally decreased with sample size for all four MSFRs in both full factorial and pairwise experimental designs (see Fig. 6 for medium noise, Figs. S13-S15 for all levels). As in the two-prey scenarios, noise in the data increased errors, and in the high noise scenarios their decrease with sample size was only small (Fig. S15). Parameter estimates were generally better when using the pairwise experimental design for Holling-2, Yodzis-FR and the Generalized-FR, while they were slightly worse than the full factorial design for Holling-3. We here support the use of pairwise experiments, which may be logistically more feasible than feeding trials involving three prey species.

Empirical datasets

Of the 23 datasets the Holling-2 MSFR was the best fitting model 15 times, followed by Holling-3 (5 times) and Yodzis-FR (3 times), see Table S1 and [Zenodo]. Switching was observed in 5 datasets, i.e. the relative proportion of eaten prey switched from avoidance to preference (see e.g. Fig. 7c). Interestingly, all of these 5 datasets were best described by the Holling-3. All 3 of the best-fitting Yodzis-FRs did not include switching, but multi-prey consumption differed from single-prey consumption through preferences $w_1 \neq w_2$ of one species over the other. None of the datasets were best described by our new Generalized-FR, meaning it did not show a difference in performance over

another model of more than 2 standard deviations (associated uncertainty). However, in 9 cases it performed as well as the best fitting model under uncertainty, but a less complex model was chosen due to the principle of parsimony. This was also the case for Yodzis-FR (8 times) and Holling-3 (13 times).

In 5 datasets, where experimental duration differed substantially between single- and multi-prey feeding trials (e.g., 24h vs. 3h), none of the models could fit all observed data sufficiently. Observed feeding rates (averaged by time) were systematically lower in long than in short experiments. Thus, modeled feeding rates tended to systematically overpredict observed feeding in the longer single-prey trials and underpredict in shorter multi-prey trials, even though our fitting method explicitly accounted for the individual duration of each trial. We assume that experimental conditions were not constant (e.g. predator hunger levels, or additional resting times) and fitting models that do not account for this to data with substantial variation in experimental duration could lead to biased parameter estimates.

We here showcase the analysis of one dataset from (Cuthbert et al., 2019), with a native cyclopoid copepod feeding on the invasive Asian tiger mosquito (prey 1) and a representative native common house mosquito (prey 2). They used a "triangle" design and conducted 65 feeding trials (6 hours without prey replacement, each). We identified Holling-2 as the best fitting model (Fig. 7). The predator shows a preference for prey 1 due to differences in attack rates (posterior $a_1 - a_2 = 1.11$ with a 95% credible interval [0.23,2.31]), but not in handling times ($h_1 - h_2 = 0.03$ [-0.05,0.11]). It was pointed out in the original study that the predator's preference might mitigate the invasive species' superior competitive ability and facilitate coexistence with native prey (as has been observed in nature). With our fully parameterized MSFR, these mechanisms could be explored more thoroughly by modeling community dynamics.

Discussion

We explored previously neglected topics in empirical MSFR research: experimental design and prey depletion. We introduced a flexible framework for parameterizing MSFR models from both single-prey and multi-prey feeding trials simultaneously and demonstrated its application thoroughly. Using ODE simulations to compute model predictions allows correcting for prey depletion during the course of the experiments, which is necessary if eaten prey are not constantly replaced (and would involve an extensive logistical effort and might disturb the predator's foraging process). Although not tested here, ODE simulations could be easily extended to include processes such as prey mortality or growth if required (Daugaard et al., 2019; Rosenbaum & Rall, 2018). If, however, experiments are conducted with prey replacement, they can be fitted through direct predictions from MSFR models (without ODE simulation). A Bayesian approach even allows using mixed datasets from experiments with and without replacement, as demonstrated here in empirical datasets and the tutorial. Furthermore, Bayesian inference quantifies uncertainty in parameters estimates exactly through posterior probability distributions of parameter estimates. Also, uncertainty in model comparison (LOO-CV) is accounted for correctly, which was previously not possible with approaches such as maximum likelihood and AIC, e.g., as used in (Stouffer & Novak, 2021).

We comprehensively tested the identifiability of four MSFR models with realistically simulated feeding trials for different noise levels, numbers of feeding trials, and experimental designs. As practical advice, we recommend a log-spaced grid design for experimental planning, which distributes more feeding trials at low abundances of individual prey species and fewer at high total prey abundances, and also multi-prey trials at different levels of total prey abundances. It produced the most accurate parameter estimates across all models, sample sizes, and noise levels. This is an extension of results from (Uszko et al., 2020), who found that log-spaced distances of abundances were more effective than an equidistant design in single-prey experiments. Additionally, for three-prey systems, we found that pairwise trials with two prey species each (which might be logistically less demanding) produce more accurate estimates than trials with all species present. Classically, two-prey experiments have often been conducted using a 'triangle' design with

single-prey trials for each species and multi-prey trials along a fixed number of total prey offered but varying prey composition (Table S1). Prey switching was then investigated via GLMs, but these studies were not able to parameterize a full MSFR model. With our approach, switching can be detected through model comparison and visualization of model predictions, and the best-fitting MSFR model can be used for dynamical modeling of species communities and hypothesis testing, e.g. effects of allometry or temperature (Gauzens et al., 2021; Kalinkat et al., 2011).

Although we have only discussed four MSFR models here, these cover important properties such as no, passive and active switching in multi-prey scenarios, as well as type 2 and type 3 behavior in single-prey scenarios. Furthermore, our proposed Generalized-FR represents a flexible but tractable model that generalizes the three other models by using focal species density-dependent attack rates $a_i(N_i)$ and community density-dependent selection factors $p_i(N_1 \ldots N_m)$ (Koen-Alonso & Yodzis, 2005). It also includes the three MSFRs when respective exponents r or q, or both, are set to zero. While a plethora of models have been proposed (Baudrot et al., 2016; Gentleman et al., 2003; Lehtinen et al., 2023; Morozov & Petrovskii, 2013), to our knowledge this is the first MSFR that combines sigmoidal behavior in single-prey scenarios, active switching in multi-prey scenarios, and species-specific handling times. An MSFR with the first two properties was proposed by (Baudrot et al., 2016), but an extension of their model H3.2 to include individual handling times in their supplement contained an error (see SI for a correction). As the strength of switching (expressed through MSFR exponents) can affect stability and coexistence (Archibald et al., 2023), active switching models such as Yodzis-FR or Generalized-FR should be considered and tested against data. This often requires allowing prey species-specific maximum feeding rates, and therefore handling times (as demonstrated in empirical datasets here).

All four models can produce feeding that is suboptimal (an increase in one prey species can lead to a decline of total feeding) or antagonistic (total feeding is lower in a mixed-prey scenario than in a single-prey scenario with identical total abundance), either through a difference in handling times or as a result of prey switching (Gentleman et al., 2003). (Vallina et al., 2014) proposed a phenomenological Kill-the-winner model as a remedy to achieve optimal feeding including prey

switching. However, this comes at the cost of identical handling times and synergistic feeding (a counterintuitive pattern, where an increase in alternative prey abundance can increase focal prey feeding) (Archibald et al., 2023). In general, it is not clear whether experimentally measured feeding is necessarily optimal (Griffen, 2021), and processes that might lead to optimal or suboptimal feeding remain to be empirically tested in the MSFR framework.

Other studies have found evidence against the Holling-2 MSFR in empirical data. In (Stouffer & Novak, 2021), a generalized Holling-2 model included parameters describing the effect of alternative prey on the feeding rate of a focal species. It outperformed the classical Holling-2 model in terms of AIC in their database of 30 experiments. Also, (Smith & Smith, 2020) found a predominance of Holling-3 over Holling-2 in field data of 48 predator size categories of fish. Here, we identified Holling-2 as the best fitting model in 15 out of 23 datasets. However, this choice was mostly conservative, as in 14 datasets other models were ranked equally under model uncertainty and Holling-2 was chosen only on the principle of parsimony. We therefore advocate for a hypothesis-driven approach when selecting model candidates for model comparison (e.g., switching vs. non-switching, or optimal vs. suboptimal).

There are some general limitations to fitting MSFR data from experiments, which however are not specific to multi-prey data, but also apply to single-prey experiments. If individual predators' traits vary strongly between feeding trials, we have shown that parameter estimates can be biased. Jensen's inequality, which states in this context that the population-level mean feeding rate $F(\bar{\theta})$ ($\bar{\theta}$ population-level mean trait) can be different from the mean of individual feeding rates $\overline{F(\theta)}$ (θ collection of individual trait values), is still an unresolved problem (Bolnick et al., 2011). If predator individuals are reused in multiple feeding trials, mixed effects models with predator ID as a random factor could account for intraspecific variation to reduce bias. However, if individual predators are used for each trial (or identity was not recorded in the experiment), this is not feasible, and our study at least quantifies the expected direction and strength of these biases.

Another problem was that some empirical datasets used a wide range of experimental duration up to a factor of 8 (mostly between single-prey and multi-prey trials). Here, a joint model

that fits all feeding trials simultaneously may be inappropriate, even if model predictions explicitly include duration. In longer experiments, non-foraging behavior becomes more likely (e.g. reduced hunger levels, resting times) (Griffen, 2021), and longer trials produce smaller estimates of attack rates and longer estimates of handling times (Li et al., 2018). We therefore suggest the use of identical trial durations when aiming to parameterise a functional response model. (Griffen, 2021) argued that it should be long enough to include non-foraging behavior, which could facilitate scaling up functional responses to realistic (field) settings. Again, prey replacement would be even more labour intensive in longer experiments, and our approach corrects for prey depletion in less costly long experiments without prey replacement.

Filling the gap between experimental evidence for single- and for multi-prey functional responses will be a challenging and lengthy endeavor. We wanted to facilitate this task by equipping researchers with the right statistical tools and also practical considerations for experimental planning. We hope that the methods we proposed will pave the way for more empirical research on predators feeding on multiple resources, thus improving the mechanistic understanding of trophic interactions in complex ecosystems.

Data and code availability

Tutorial and ready-to-use R code available via Github, also code and results for analysis of empirical data: https://github.com/benjamin-rosenbaum/multispecies_functional_responses
This repository will be archived via Zenodo upon acceptance. A full list of public data used in this study is presented in Table S1.

Acknowledgements

We gratefully acknowledge the support of iDiv funded by the German Research Foundation (DFG-FZT 118, 202548816). The scientific results have in part been computed at the High-Performance Computing Cluster EVE of the Helmholtz Centre for Environmental Research

(UFZ) and iDiv, and we thank Christian Krause for technical support. We thank Ross Cuthbert for making additional data openly available.

Conflict of interest statement

We declare no conflict of interest.

References

Abrams, P. A. (2022). Food web functional responses. *Frontiers in Ecology and Evolution*, *10*, 984384.

Archibald, K. M., Sosik, H. M., Moeller, H. V., & Neubert, M. G. (2023). Predator switching strength controls stability in diamond-shaped food web models. *Journal of Theoretical Biology*, *570*, 111536.

Baudrot, V., Perasso, A., Fritsch, C., Giraudoux, P., & Raoul, F. (2016). The adaptation of generalist predators' diet in a multi-prey context: insights from new functional responses. *Ecology*, *97*(7), 1832–1841.

Beardsell, A., Gravel, D., Clermont, J., Berteaux, D., Gauthier, G., & Bêty, J. (2022). A mechanistic model of functional response provides new insights into indirect interactions among arctic tundra prey. *Ecology*, e3734.

Bolnick, D. I., Amarasekare, P., Araújo, M. S., Bürger, R., Levine, J. M., Novak, M., Rudolf, V. H. W., Schreiber, S. J., Urban, M. C., & Vasseur, D. A. (2011). Why intraspecific trait variation matters in community ecology. *Trends in Ecology & Evolution*, *26*(4), 183–192.

Brose, U., Archambault, P., Barnes, A. D., Bersier, L.-F., Boy, T., Canning-Clode, J., Conti, E., Dias, M., Digel, C., Dissanayake, A., Flores, A. A. V., Fussmann, K., Gauzens, B., Gray, C., Häussler, J., Hirt, M. R., Jacob, U., Jochum, M., Kéfi, S., … Iles, A. C. (2019). Predator traits determine food-web architecture across ecosystems. *Nature Ecology & Evolution*, 1.

Chesson, J. (1983). The estimation and analysis of preference and its relationship to foraging models. *Ecology*, *64*(5), 1297–1304.

Coblentz, K. E. (2020). Relative prey abundance and predator preference predict individual diet variation in prey-switching experiments. *Ecology*, *101*(1), e02911.

Cuthbert, R. N., Callaghan, A., & Dick, J. T. A. (2019). A novel metric reveals biotic resistance potential and informs predictions of invasion success. *Scientific Reports*, *9*(1), 15314.

Daugaard, U., Petchey, O. L., & Pennekamp, F. (2019). Warming can destabilize predator-prey interactions by shifting the functional response from Type III to Type II. *The Journal of Animal Ecology*, *88*(10), 1575–1586.

DeLong, J. P. (2021). *Predator Ecology: Evolutionary Ecology of the Functional Response*. Oxford University Press.

DeLong, J. P., Uiterwaal, S. F., & Dell, A. I. (2021). Trait-Based Variation in the Foraging Performance of Individuals. *Frontiers in Ecology and Evolution*, *9*, 649542.

Dutang, C., & Savicky, P. (2023). *randtoolbox: Generating and Testing Random Numbers*.

Fenlon, J. S., & Faddy, M. J. (2006). Modelling predation in functional response. *Ecological Modelling*, *198*(1), 154–162.

Gauzens, B., Brose, U., Delmas, E., & Berti, E. (2023). *ATNr*: Allometric Trophic Network models in R. *Methods in Ecology and Evolution*, *14*(11), 2766–2773.

Gauzens, B., Rosenbaum, B., Kalinkat, G., Boy, T., Jochum, M., Kortsch, S., O'Gorman, E. J., & Brose, U. (2021). Adaptive foraging behaviour increases vulnerability to climate change. In *bioRxiv*. https://doi.org/10.1101/2021.05.05.442768

Gentleman, W., Leising, A., Frost, B., Strom, S., & Murray, J. (2003). Functional responses for zooplankton feeding on multiple resources: a review of assumptions and biological dynamics. *Deep-Sea Research. Part II, Topical Studies in Oceanography*, *50*(22), 2847–2875.

Griffen, B. D. (2021). Considerations When Applying the Consumer Functional Response Measured Under Artificial Conditions. *Frontiers in Ecology and Evolution*, *9*, 461.

Holling, C. S. (1959). Some Characteristics of Simple Types of Predation and Parasitism. *The Canadian Entomologist*, *91*(7), 385–398.

Holt, R. D. (1983). Optimal Foraging and the Form of the Predator Isocline. *The American Naturalist*, *122*(4), 521–541.

Jeschke, J. M., Kopp, M., & Tollrian, R. (2002). Predator functional responses: Discriminating between handling and digesting prey. *Ecological Monographs*, *72*(1), 95.

Jeschke, J. M., Kopp, M., & Tollrian, R. (2004). Consumer-food systems: why type I functional responses are exclusive to filter feeders. *Biological Reviews of the Cambridge Philosophical Society*, *79*(2), 337–349.

Kalinkat, G., Rall, B. C., Uiterwaal, S. F., & Uszko, W. (2023). Empirical evidence of type III functional responses and why it remains rare. *Frontiers in Ecology and Evolution*, *11*, 1033818.

Kalinkat, G., Rall, B. C., Vucic-Pestic, O., & Brose, U. (2011). The allometry of prey preferences. *PloS One*, *6*(10), e25937.

Koen-Alonso, M. (2007). A Process-Oriented Approach to the Multispecies Functional Response. In N. Rooney, K. S. McCann, & D. L. G. Noakes (Eds.), *From Energetics to Ecosystems: The Dynamics and Structure of Ecological Systems* (pp. 1–36). Springer Netherlands.

Koen-Alonso, M., & Yodzis, P. (2005). Multispecies modelling of some components of the marine community of northern and central Patagonia, Argentina. *Canadian Journal of Fisheries and Aquatic Sciences. Journal Canadien Des Sciences Halieutiques et Aquatiques*, *62*(7), 1490–1512.

Kratina, P., Rosenbaum, B., Gallo, B., Horas, E. L., & O'Gorman, E. J. (2022). The Combined Effects of Warming and Body Size on the Stability of Predator-Prey Interactions. *Frontiers in Ecology and Evolution*, *9*, 947.

Lehtinen, S. O., Perälä, T. A., Uusi-Heikkilä, S. K., & Kuparinen, A. K. (2023). Mutually exclusive feeding yields Holling type III functional response. *Functional Ecology*. https://doi.org/10.1111/1365-2435.14475

Li, Y., Rall, B. C., & Kalinkat, G. (2018). Experimental duration and predator satiation levels systematically affect functional response parameters. *Oikos* , *127*(4), 590–598.

Lotterhos, K. E., Fitzpatrick, M. C., & Blackmon, H. (2022). Simulation Tests of Methods in Evolution, Ecology, and Systematics: Pitfalls, Progress, and Principles. *Annual Review of Ecology, Evolution, and Systematics*, *53*(1), 113–136.

Martinez, N. D. (2020). Allometric Trophic Networks From Individuals to Socio-Ecosystems: Consumer–Resource Theory of the Ecological Elephant in the Room. *Frontiers in Ecology and Evolution*, *8*, 92.

McCard, M., South, J., Cuthbert, R. N., Dickey, J. W. E., McCard, N., & Dick, J. T. A. (2021). Pushing the switch: functional responses and prey switching by invasive lionfish may mediate their ecological impact. *Biological Invasions*, *23*(6), 2019–2032.

Morozov, A., & Petrovskii, S. (2013). Feeding on multiple sources: towards a universal parameterization of the functional response of a generalist predator allowing for switching. *PloS One*, *8*(9), e74586.

Murdoch, W. W. (1969). Switching in general predators: Experiments on predator specificity and stability of prey populations. *Ecological Monographs*, *39*(4), 335–354.

Murdoch, W. W., & Oaten, A. (1975). Predation and Population Stability. In A. MacFadyen (Ed.), *Advances in Ecological Research* (Vol. 9, pp. 1–131). Academic Press.

Pritchard, D. W., Paterson, R. A., Bovy, H. C., & Barrios-O'Neill, D. (2017). frair: an R package for fitting and comparing consumer functional responses. *Methods in Ecology and Evolution*, *8*(11), 1528–1534.

Rosenbaum, B., & Rall, B. C. (2018). Fitting functional responses: Direct parameter estimation by simulating differential equations. *Methods in Ecology and Evolution* , *9*(10), 2076–2090.

Ryabov, A. B., Morozov, A., & Blasius, B. (2015). Imperfect prey selectivity of predators promotes biodiversity and irregularity in food webs. *Ecology Letters*, *18*(11), 1262–1269.

Smith, B. E., & Smith, L. A. (2020). Multispecies functional responses reveal reduced predation at high prey densities and varied responses among and within trophic groups. *Fish and Fisheries* , *21*(5), 891–905.

Soetaert, K., Petzoldt, T., & Setzer, R. W. (2010). Solving Differential Equations in R: Package deSolve. *Journal of Statistical Software*, *33*, 1–25.

Sohlström, E. H., Archer, L. C., Gallo, B., Jochum, M., Kordas, R. L., Rall, B. C., Rosenbaum, B., & O'Gorman, E. J. (2021). Thermal acclimation increases the stability of a predator-prey interaction in warmer environments. *Global Change Biology*, *27*(16), 3765–3778.

Stan Development Team. (2023). *RStan: the R interface to Stan*. https://mc-stan.org/

Stouffer, D. B., & Novak, M. (2021). Hidden layers of density dependence in consumer feeding rates. *Ecology Letters*, *24*(3), 520–532.

Uiterwaal, S. F., Lagerstrom, I. T., Lyon, S. R., & DeLong, J. P. (2022). FoRAGE database: A compilation of functional responses for consumers and parasitoids. *Ecology*, *103*(7), e3706.

Uszko, W., Diehl, S., Englund, G., & Amarasekare, P. (2017). Effects of warming on predator-prey interactions - a resource-based approach and a theoretical synthesis. *Ecology Letters*, *20*(4), 513–523.

Uszko, W., Diehl, S., & Wickman, J. (2020). Fitting functional response surfaces to data: a best practice guide. *Ecosphere* , *11*(4), 463.

Vallina, S. M., Ward, B. A., Dutkiewicz, S., & Follows, M. J. (2014). Maximal feeding with active prey-switching: A kill-the-winner functional response and its effect on global diversity and biogeography. *Progress in Oceanography*, *120*, 93–109.

Vehtari, A., Gabry, J., Magnusson, M., Yao, Y., Bürkner, P.-C., Paananen, T., & Gelman, A. (2023). *loo: Efficient leave-one-out cross-validation and WAIC for Bayesian models*. https://mc-stan.org/loo/

Williams, R. J., & Martinez, N. D. (2004). Stabilization of chaotic and non-permanent food-web dynamics. *The European Physical Journal. B*, *38*(2), 297–303.

Zurell, D., Berger, U., Cabral, J. S., Jeltsch, F., Meynard, C. N., Münkemüller, T., Nehrbass, N., Pagel, J., Reineking, B., Schröder, B., & Grimm, V. (2010). The virtual ecologist approach: simulating data and observers. *Oikos* , *119*(4), 622–635.

Figures

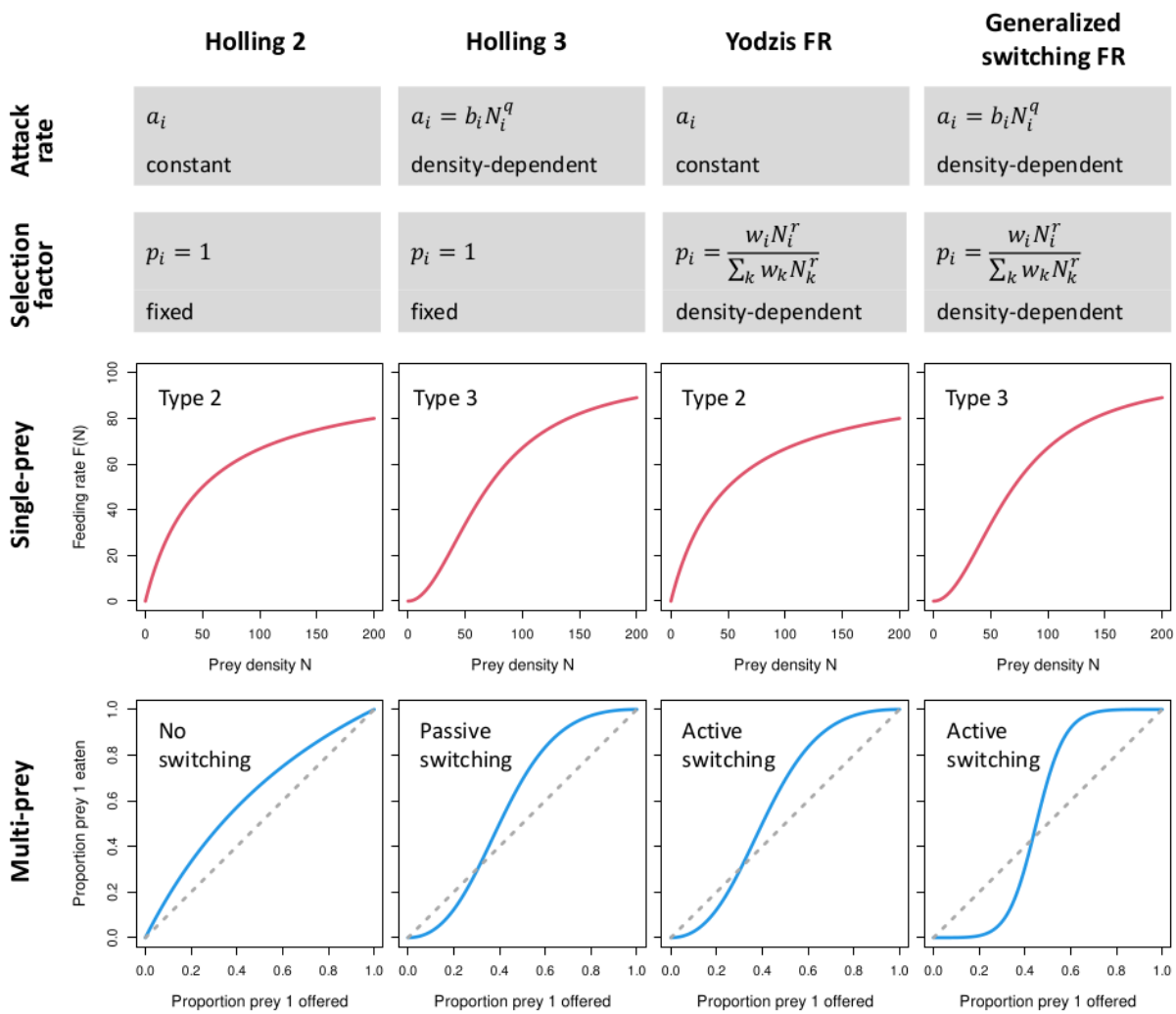

Figure 1: Four MSFR models of the general formulation as in eq. 2 with attack rates a_i and selection factors p_i either constant or density-dependent. In single-prey scenarios, they collapse to a type 2 or type 3 FR. In multi-prey scenarios, prey preference and switching can be passive (as predicted from single-prey scenarios) or active (distinct or more pronounced than in single-prey scenarios).

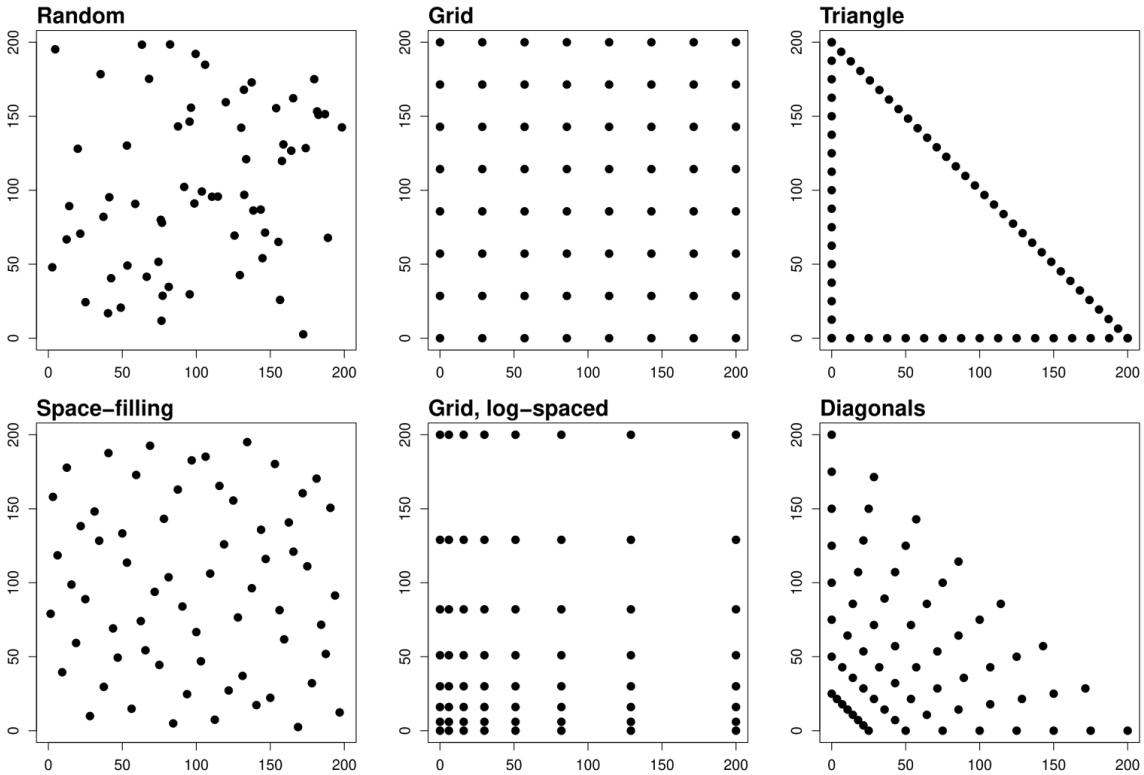

Figure 2: Six experimental designs for offered numbers of prey (N_1, N_2) for two-prey experiments with a maximum initial abundance of 200. Sample size *n*=64, each.

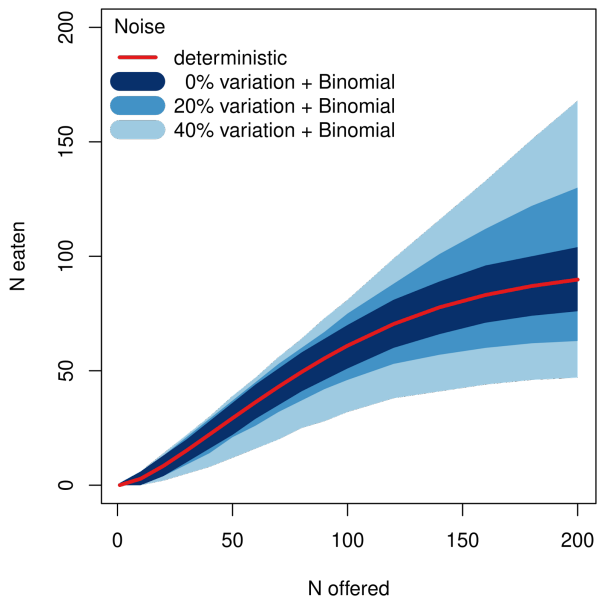

Figure 3: 95% quantiles of simulated data for a single-species Holling-3 FR ($b = 0.04$, $h = 0.01$, $q = 1.0$) depending on the level of predator trait variation.

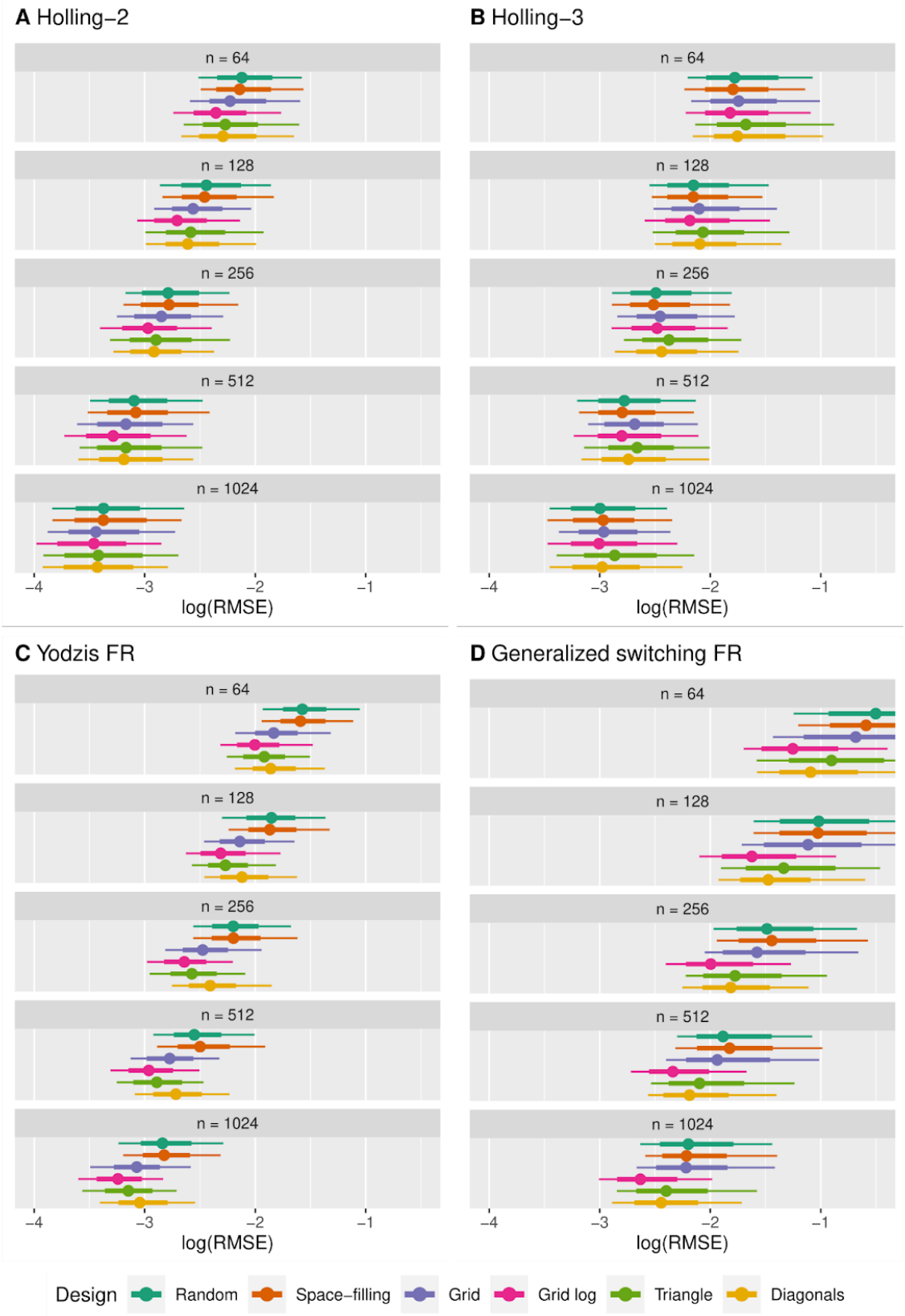

Figure 4: Distributions of relative RMSE vs. experimental design and sample size, noise level: medium. 500 datasets each. Dots represent means, bold lines are 66% quantiles, thin lines are 95% quantiles.

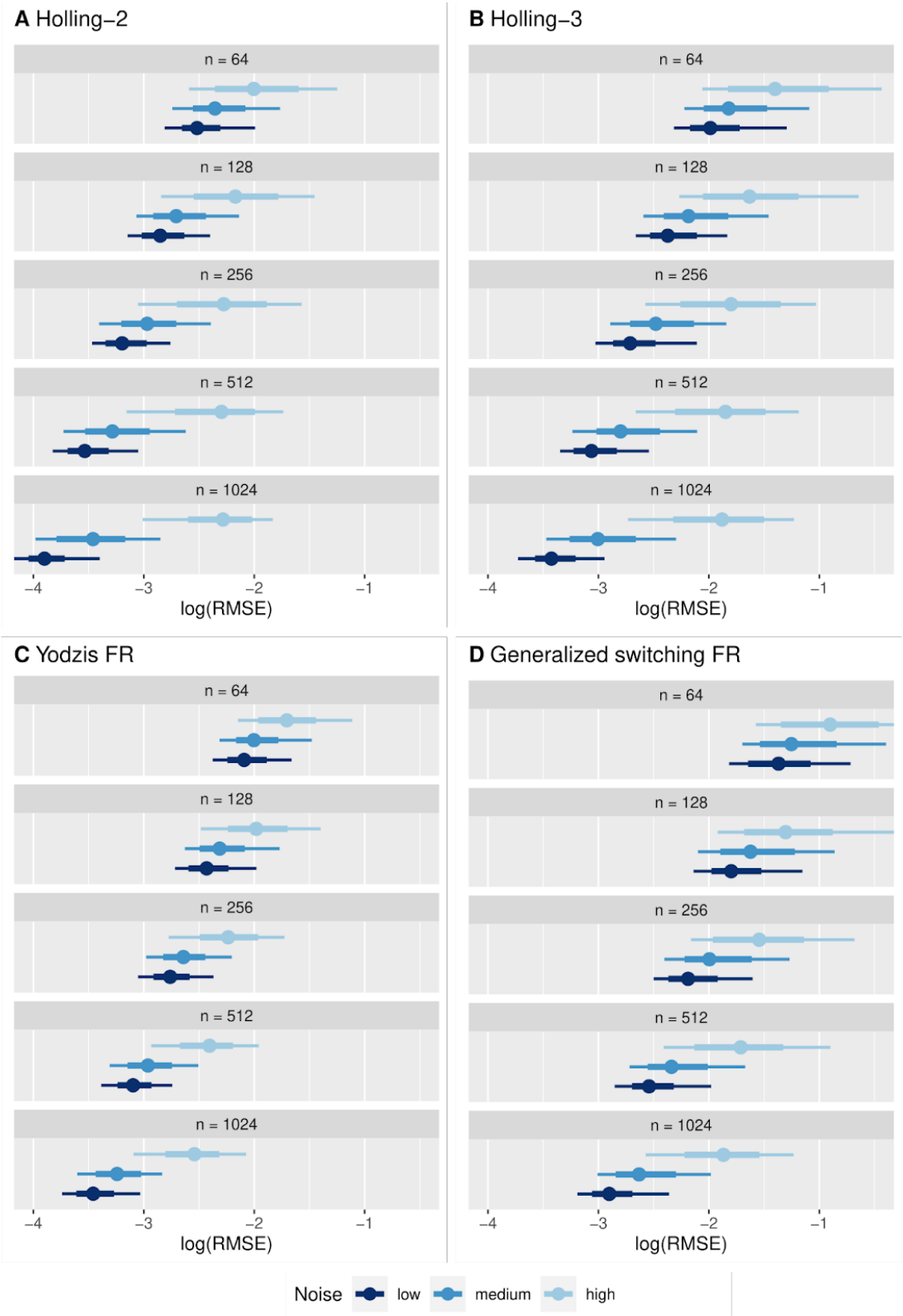

Figure 5: Distributions of relative RMSE vs. noise and sample size, design: log-spaced grid. 500 datasets each. Dots represent means, bold lines are 66% quantiles, thin lines are 95% quantiles.

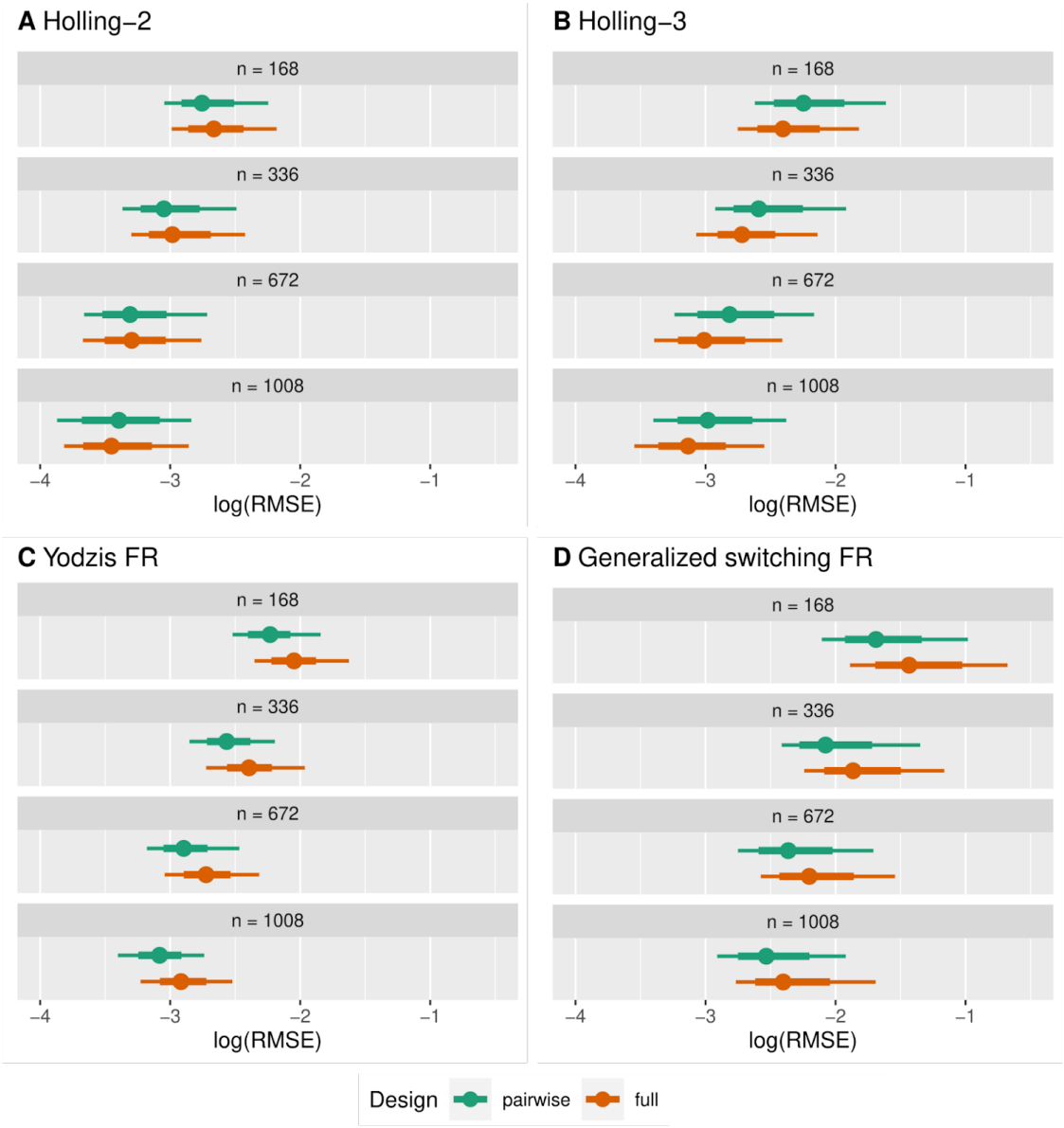

Figure 6: Three-prey scenarios. Distributions of relative RMSE vs. experimental design and sample size, noise level: medium. 500 datasets each. Dots represent means, bold lines are 66% quantiles, thin lines are 95% quantiles.

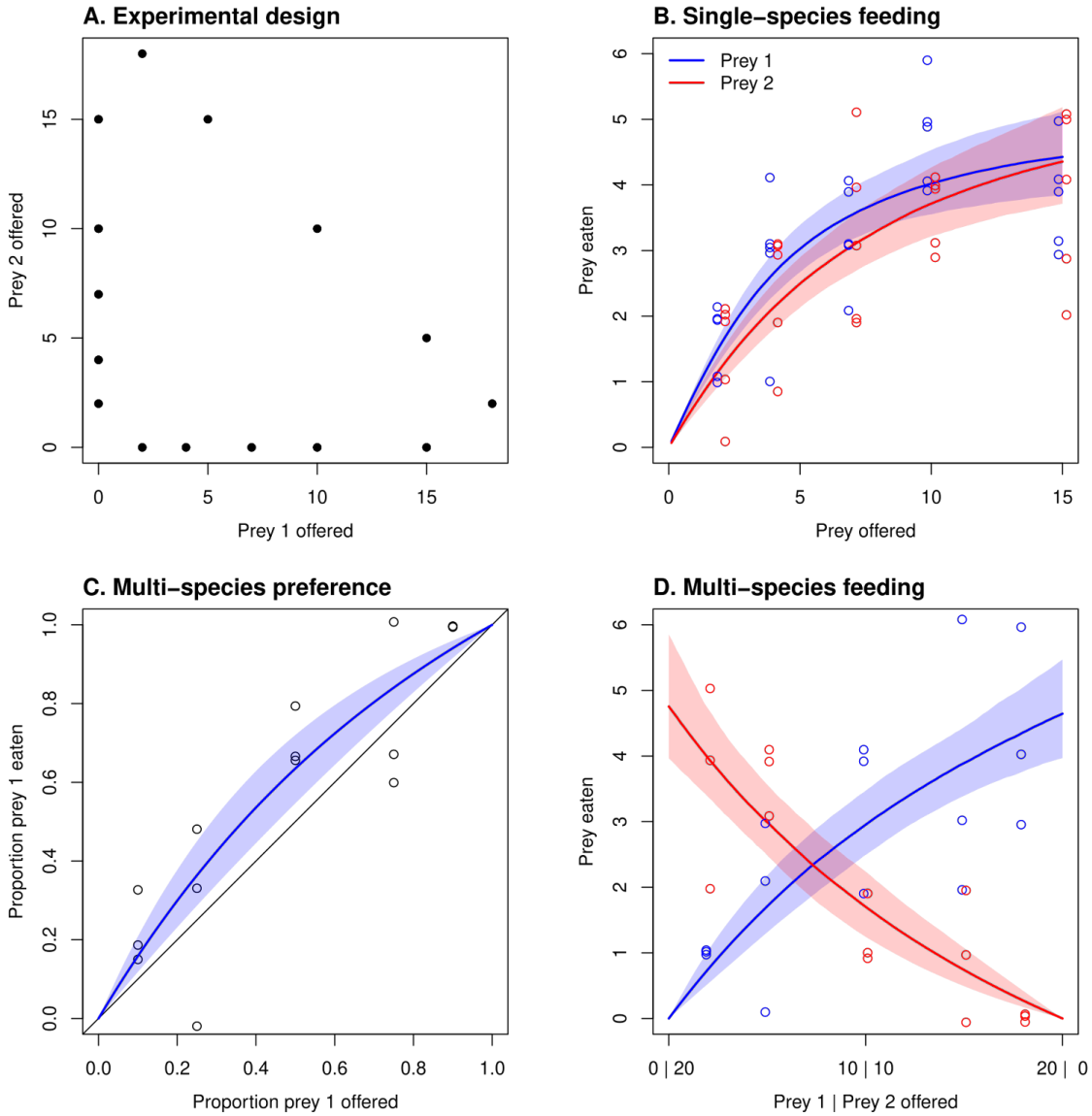

Figure 7: Best-fitting model Holling-2 for empirical data from (Cuthbert et al., 2019). (A) Experimental design ("Triangle") with 3 replicates per single-species and 5 replicates per multi-species combinations, each. (B) Single-species observed and predicted eaten prey (line is median, shaded areas 90% credible intervals). Multi-species observed and predicted for (C) proportion of prey 1 eaten $\frac{N_{E,1}}{N_{E,1}+N_{E,2}}$ vs. proportion of prey 1 offered $\frac{N_{0,1}}{N_{0,1}+N_{0,2}}$, and (D) eaten prey along the diagonal (panel A top-left to bottom-right, $N_{0,1} + N_{0,2} = 20$).